Nat Hazards (2013) 68:915–927
DOI 10.1007/s11069-013-0665-3

ORIGINAL PAPER

# Extracting desertification from Landsat TM imagery based on spectral mixture analysis and Albedo-Vegetation feature space

**Jinghu Pan · Tianyu Li**

Received: 25 January 2013 / Accepted: 25 March 2013 / Published online: 2 April 2013
© Springer Science+Business Media Dordrecht 2013

**Abstract** Land desertification has been a worldwide environmental problem. Desertification monitoring and evaluation are very important content in desertification context. Scientific and accurate evaluation of desertification can provide scientific basis for decision making in mitigating desertification. Because of the advantage of large amount of information, short cycle and broad scope of data, less restrictions on the human and material resources and so on, remote sensing has become an important technology to monitor land desertification in the past 30 years. Desertification is the most typical and serious form of desertification in China, especially in the oasis zone distributed along inland rivers or in the lower reaches of inland rivers in northwestern China. Quantitative evaluation of the current desertification remote sensing methods used is mostly obtained through the vegetation index and vegetation cover, to gain information on the extent of desertification. As the arid and semiarid sparse vegetation cover, soil and soil moisture on the most common vegetation index have a greater effect. First, based on the spectral mixture analysis model, three kinds of endmember consisting of vegetation, water and bare soil were selected. The image dimensionality was reduced by the minimum noise fraction (MNF). The pixel purity index transformation was used to narrow the range of the endmember. On the scatter plot of MNF, three kinds of endmember were selected, and relative abundance distribution of each component was obtained by using linear spectral mixture model. Second, a spectral feature space composed of vegetation component and land surface albedo retrieved from Landsat TM Imagery was constructed to evaluate desertification present condition and degree quantificationally. Last, an empirical study was carried out taking the middle reaches of Heihe River as an example. Results indicated that this method makes full use of multi-dimensional remote sensing information, reflecting the desertification land cover, water, thermal environment and its changes, with a clear biophysical significance, and the index is

J. Pan (✉)
College of Geographic and Environmental Science, Northwest Normal University,
967 Anning East Road, Lanzhou 730070, People's Republic of China
e-mail: panjh-nwnu@163.com

T. Li
College of Geographic Science, Nanjing Normal University, Nanjing 210046, China
e-mail: 55890345@qq.com

simple, easy to obtain, high precision, and is conducive to quantitative analysis, monitoring and desertification assessment of desertification. It was rather ideal to assess desertification on the basis of Albedo-Vegetation feature space: correct prediction proportion of testing samples reached 90.3 %. This method was beneficial to the desertification quantitative analysis and monitoring with the characteristics of simple index, easy accessibility and high accuracy.

**Keywords** Desertification evaluation · Remote sensing · Spectral mixture analysis · Albedo-Vegetation feature space · Heihe River

## 1 Introduction

Desertification is a general process of surface environmental degradation under the combined effect of natural and human actions, the essence of which is to weaken or lose the ability of land to grow green plants (Ibrahim 1978; Hellden 1991). The evaluation research of desertification is one of the core contents in the desertification research field. In the past 30 years, remote sensing technology with its advantages of widely observational range, abundant information, quickly updated data and high precision was used widely in the research of desertification evaluation (Smith et al. 1990; Diouf and Lambin 2001; Yan et al. 2009; Santini et al. 2010; Xu et al. 2010). At present, most methods used in remote sensing quantitative evaluation of desertification mainly get information about vegetation coverage and desertification degree by calculating vegetation index (Malo and Nicholson 1990; Paisley et al. 1991; Chen et al. 1998; Nicholson et al. 1998; Chopping et al. 2008; Hanafi and Jauffret 2008; Xue et al. 2009).

The arid region is characterized by its scarce precipitation and intensive evaporation which lead to sparse growth of vegetations and simple structure of plant groups. Given this situation, the spectral characteristics of vegetation in these regions do not have apparent absorption valleys and reflection peaks which are not identical with plants in healthy status and thus makes it a tough task to have spectral analysis of vegetation owing to its feeble signals in satellite imagery. When the study area being covered by extremely low vegetation coverage, the spatial resolution of vegetation in these areas cannot support the traditional vegetation index (NDVI, LAI, etc.) serving as an effective way for extracting vegetation information. It is reported that the application of LSMA (linear spectral mixture analysis) in vegetation coverage research dealing with pixel mixture has a dependable performance in arid or semiarid area. In addition, due to the sparse vegetation coverage in arid and semiarid areas, soil and soil humidity will have a greater impact on the normalized difference vegetation index (NDVI) (Becker and Choudhury 1988; Kremer and Running 1993; Wessels et al. 2004; Huang and Siegert 2006; Hill et al. 2008). Some researchers adopt the Modified Soil Adjustment Vegetation Index (MSAVI) or the enhanced vegetation index (EVI) to eliminate the influence of soil (Li and Zhou 2001; Li et al. 2003, 2010; Wu et al. 2007). However, due to the fact that all the indexes mentioned above are very sensitive to the background color of soil, the living biomass of vegetation, to some extent, is underestimated by various vegetation indexes, although some soil adjustment factor is adopted to improve the results of evaluation (Wu and Peng 2009). The brightness values of various pixels which constitute the remote sensing image of arid and semiarid areas are the comprehensive records of various spectral characteristics of ground. To accurately obtain the information about vegetation coverage and to better evaluate desertification degree, it is better to extract vegetation information from the mixed information, and the vegetation information must be highly correlated with vegetation coverage and biomass. Consequently, spectral mixture analysis (SMA) began to be used in evaluating desertification of arid areas (Alfredo et al. 2002; Hosterta et al. 2003; Asis and Omasa 2007; Sonnenschein et al. 2011). In addition, desertification process is also affected by various human factors and some natural factors such as climate and topography. The evaluation result of a single vegetation index is more one-sided and cannot comprehensively reflect the development information of desertification. Some researchers try to quantitatively analyze and monitor desertification by establishing a quantitative relationship between desertification process and bio-physical characteristics (albedo, land surface temperature) of land surface (Tripathy et al. 1996; Zeng et al. 2005, 2006).

In this paper, we proposed a desertification monitoring model based on the relationship between desertification and a two indexes such as albedo, vegetation, as well as the spatial distribution law of desertification in Albedo-Vegetation feature space. Then, the model was applied in study area with relatively complete desertification types in the middle reaches of Heihe River. The result of the present research shows that the indexes of the model can reflect the desertification land surface cover, the water–heat combination and their changes, and it also has definite biophysical significance. The model can make full use of easy accessed multi-dimensional remote sensing information and has higher monitoring accuracy. It can easily achieve the automatic identification of land desertification.

## 2 Methods

### 2.1 Data

The study area is the areas in the middle reaches of Heihe River and its nearby regions and is located in the western part of China (Fig. 1). The mean annual temperature ranges from 8 to 10 °C, while the rainfall varies from 50 to more than 300 mm over the high mountainous areas (Fig. 1). A Landsat TM image (path 133, row 33) acquired on August 14, 2010, was used in this study. Firstly, radiometric calibration was finished. The image DN values were transformed into spectral radiance value and then into land surface albedo. For this reason, the internal errors caused by sensor were eliminated. Considering the fact that the sky over the study area was cloudless and atmosphere is homogeneous when the image was obtained, the 6S atmospheric correction model which was used widely and could not be influenced by regional characteristics and objectives types was adopted for atmosphere correction. Then, the ground control point was selected based on a 1:50,000 topographic maps. Polynomial geometric correction was conducted, and RMS error was >0.5 pixels. Based on the nearest neighbor algorithm, the image of each band was re-sampled to 30-m resolution ratio. To further enhance the accuracy of the image geometric correction, the method proposed by Civco was used here (Civco 1989). To remove the topography effect, the image was corrected by DEM of the 1:50,000 topographic maps, while the thematic maps such as geomorphology, soil, vegetation, land utilization of the study area were collected as a necessary complement for remote sensing analysis.

The following equation is used to estimate surface albedo of the study area (Liang 2000):

$$\text{Albedo} = (0.356\rho_1 + 0.130\rho_3 + 0.373\rho_4 + 0.085\rho_5 + 0.072\rho_7) - 0.0018 \qquad (1)$$

Where $\rho_n$ is the albedo of band $n$.

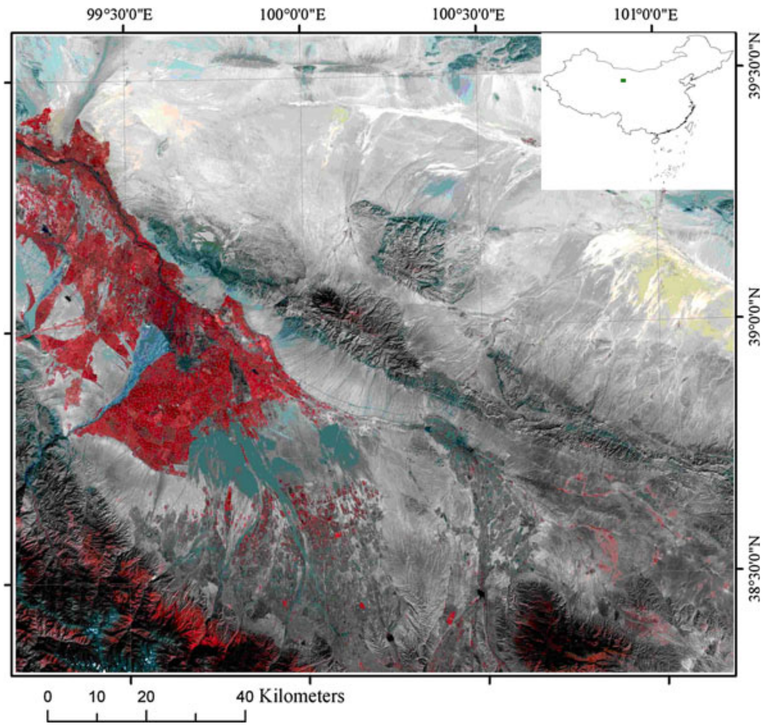


**Fig. 1** Location and topographic characteristics of the study area from a LANDSAT 5-derived image collected in August 2010

The typical sampling method is applied to the data collected in ground survey. In the pixels selected randomly, the representative ones were chosen and their coordinates were input to GPS. By navigating one by one, the precise locations of the quadrat were determined. Then, desertification (total vegetation coverage, arbor, shrub and grass coverage, soil type and soil surface morphology, etc.) of the quadrat was investigated. When the proportion of various desertification types reached 70 %, it can be concluded that the desertification type of the quadrat is correct. The area of herb quadrat is 1 $m^2$, while the combined area of shrub and herb is 100 $m^2$. The diagonal method is applied to the survey of vegetation coverage. The value of vegetation coverage is the proportion between the length of the diagonal covered by vegetation corona and the total length of it. Based on the data collected in field survey and thematic data, the comprehensive evaluation of desertification in the study area will be conducted under the conditions of considering land types, desertification types, vegetation coverage, vegetation community type, land surface morphology and the thickness of soil, etc.

## 2.2 Mixed pixel unmixing

Mixed spectrum is a combination of several pure spectrum (also known as endmember), which is used to calculate the proportion of each surface feature within a pixel. Linear spectral mixture model is the linear combination, the weight coefficients of which are the albedos of pixel components in a certain band reflected, respectively, by area proportion between each component and its pixel (Ridd 1995; Small 2001; Hosterta et al. 2003; Pu et al. 2008). Model fitting accuracy can be evaluated by root-mean-square error of m spectrum wave bands of residual. Linear spectrum mixture model extracting impervious water surface will go through the following five steps (Boardman and Kruse 1994): (1) minimum noise fraction transform (MNF). MNF is equivalent to the principle component transform of two overlap. It is an effective way to reduce dimension of multispectral and hyperspectral remote sensing images; (2) pixel purity index (PPI) calculation. PPI is the index to measure the purity of pixels. To calculate pixel purity value is better to find spectrum endmember within multi-spectral data; (3) endmember land category collection; (4) linear spectrum analysis and (5) accuracy evaluation.

## 2.3 Albedo-Vegetation feature space construction

Surface albedo retrieved from remote sensing data is physical parameters which present the reflection characteristics of surface radiation and solar shortwave radiation. Surface albedo is influenced by soil moisture, vegetation coverage, snow cover and other abnormal conditions of the land surface. The change of underlying surface influenced by desertification leads to the obvious change of surface albedo. The results of Li et al.'s fixed position observation show that grassland desertification occurs when surface albedo reaches a certain value, and the threshold of surface albedo is 0.3 (Li et al. 2006). Vegetation and albedo constitute a two-dimensional feature space (Fig. 2). The statuses of desertification under the condition of different vegetation coverage are presented in the four points A, B, C and D represent the extreme conditions of Albedo-Vegetation feature space. In the plant growing season, apart from cloud and water, all kinds of surface features are included in the quadrilateral area enclosed by the four points A, B, C and D. In the feature space, surface albedo is not only a function of the vegetation cover but also a function of soil moisture content. A–C line of the quadrilateral represents the highest albedo line, reflecting the drought conditions of the completely arid lands under the condition of the given vegetation cover degree. B–D line shows the lowest albedo line, reflecting the status of surface water.

As for desertification remote sensing monitoring, it is more convenient and easier to use a comprehensive spectral index rather than a couple of separation variables (Gillies et al. 1997). That is, to realize quantitative monitoring and investigating of spatial–temporal

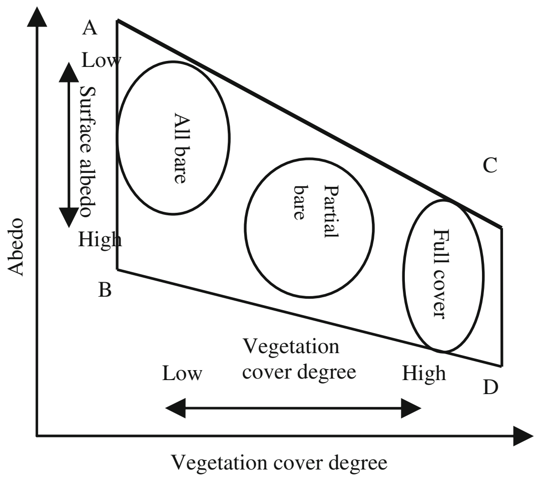


**Fig. 2** Albedo-Vegetation feature space (Zeng et al. 2006)

distribution and the dynamic variation of desertification, combination information of vegetation index and land surface albedo in A-V feature space can be used to select the reasonable indexes which reflect desertification degree and may distinguish the different desertification land. The reasonable solution of the problem, in fact, is the question how to use certain comprehensive index to distinguish A-V feature space as required. Various desertification lands can be effectively differentiated by distinguishing the A-V feature space with the vertical albedo line, while the position of the vertical line can be expressed by the simply binary linear polynomial of the A-V feature space (Verstraete and Pinty 1996).

## 3 Results and analysis

### 3.1 Results of spectral mixture analysis

Spectral mixture analysis (SMA) process is done with the help of ENVI software. Table 1 represents eigenvalues and variance contributions rate of each MNF component. Figure 3 shows the six components (MNF6 is thermal infrared band and free of decomposition) decomposed by remote image. By visual distinguishing and analyzing the eigenvalue of each component, the contribution rate of the former three MNF components to the original image reaches 95.65 % and the space texture is clear. However, the space texture of the latter three components is vague, and there is plenty of noise. Therefore, only the former three components are selected to calculate the purity index of pixels. Figure 4 is the feature space scatter diagram of the former three components.

Terminal land types can be identified by analyzing pixel types which are in the endpoint region of the scatter diagram corresponding to the original albedo image. The endpoints correspond to the plant, water body and bare soil, respectively. The determination must satisfy the conditions that the terminal land type keeps a high PPI value in their corresponding land types and in the endpoint area of the scatter diagram as well. N-dimension divergence analysis is conducted on PPI in PCA space. In the transforming process of PPI space, terminal units can be acquired from the vertex of polyhedron. The least square method is applied to a restrictive three-endmember linear spectral mixture model, and every pixel is modeled into a combination of three-endmember types. Then, the spatial distribution map (Fig. 5) of each endmember's cover degree is obtained. As shown in Fig. 5, the regions with white or light color represent the higher component abundance of the basic components in a pixel, while the regions with black or dark color represent the lower component abundance. Vegetation component image (Fig. 5a) mainly reflects the distribution status of vegetation in the research area; bare soil component image (Fig. 5c) distributing in the most part of the study area reflects the desertification distribution in a certain extent, while it should combine the albedo image to build the feature space to distinguish desertification degree, there is only a very small distribution of water body component (Fig. 5b).

**Table 1** Eigenvalue and variance contribution of each MNF component

| Component | MNF_1 | MNF_2 | MNF_3 | MNF_4 | MNF_5 | MNF_6 |
|---|---|---|---|---|---|---|
| Feature value | 384.724 | 62.706 | 21.346 | 13.016 | 5.735 | 2.546 |
| Contribute rate (%) | 78.50 | 12.80 | 4.36 | 2.66 | 1.17 | 0.52 |

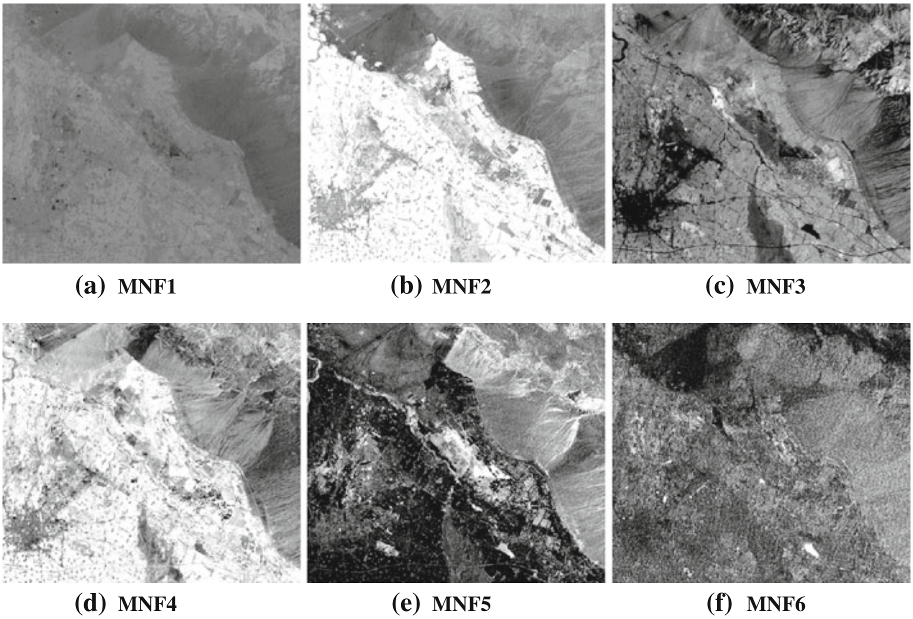


**Fig. 3** Components of MNF (partial region)

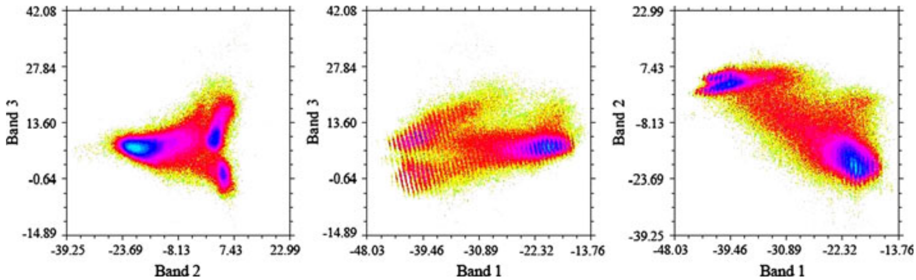


**Fig. 4** Feature space scatter diagram of the former three-component endmembers

According to the decomposition results, the mean value of total mean-square deviation must be within 0.02 (Yuan and Marvin 2007). Based on the statistics of mean-square deviation images, the maximum value of RMS is 0.00077, the minimum value 0 and mean value 0.00009. All the results much >0.02 are satisfied with the accuracy requirement. It can be seen that the number of terminal land types selected for this study from the quantitative aspect is suitable, spectrum of the terminal land types is precise and decomposition precise is high. Therefore, the decomposition results of the study are reliable.

### 3.2 Desertification information extracting from A-V feature space

In order to investigate the transformation of desertification in two-dimension feature space constituted by vegetation component and albedo, the scatter diagram of Albedo-Vegetation feature space is constructed by the typical districts which almost contain all the soil surface

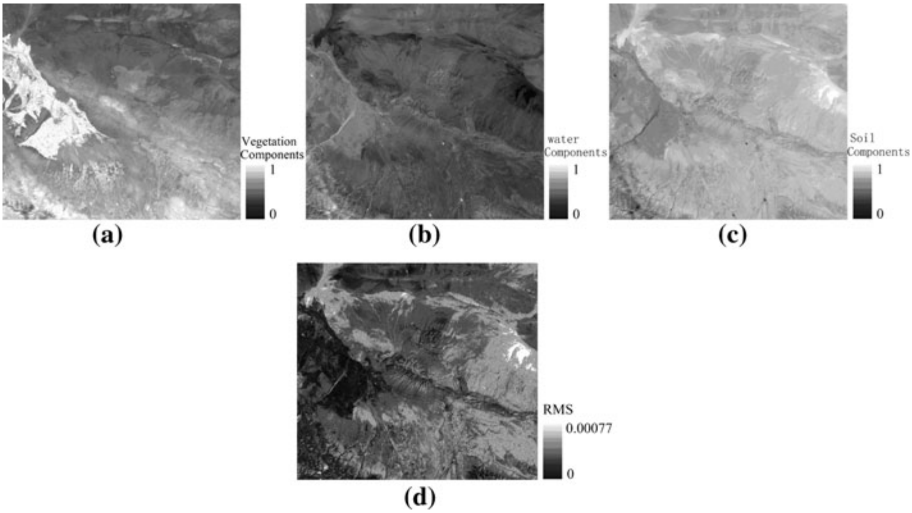


**Fig. 5** Coverage of three-endmember and RMS distribution

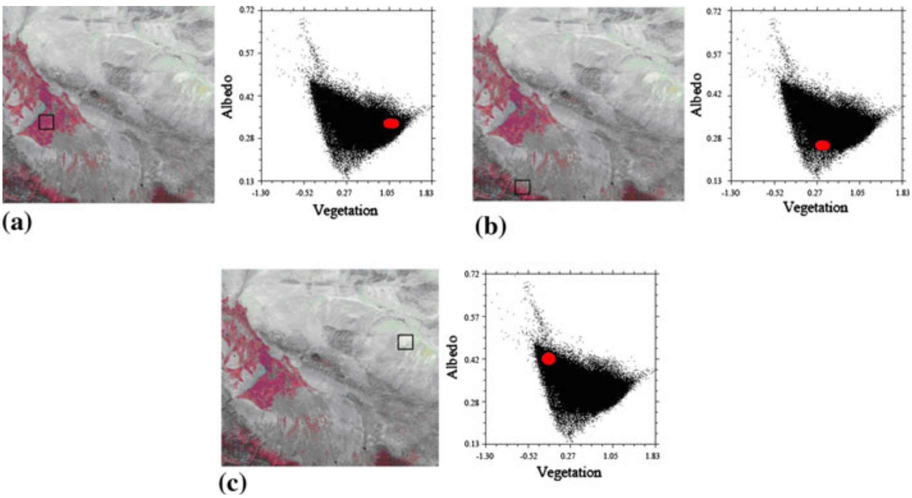


**Fig. 6** Comparison between different land coverage types and Albedo-Vegetation feature space (**a** all vegetation cover, **b** partial vegetation cover, **c** all bare)

coverage types of the study area and the vegetation components which are decomposed by soil surface albedo and mixture spectrum. Each soil surface coverage type in A-V feature space has its prominently distinctive change. Figure 6 presents the distributions of the different soil surface coverage types in A-V feature space and their corresponding image features. Different soil surface coverage type can be distinguished well in the feature space.

In order to acquire the quantitative relationship between albedo of different desertification land and vegetation, statistical regression analysis is conducted on the raster graphic of albedo and vegetation with the help of grid regression function of ArcGIS; 350 points distributing in the different land with the different desertification degree are selected

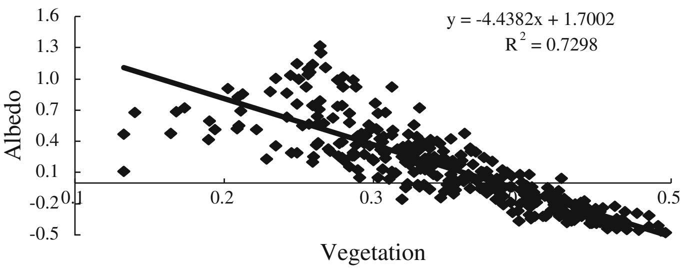


**Fig. 7** Regression analysis of Albedo-Vegetation

randomly and analyzed. The result (Fig. 7) shows that there is a significantly negative linear correlation between vegetation and albedo corresponding to different desertification land types. Regression equation is as follows:

$$\text{Albedo} = -4.4382\text{Vegetation} + 1.7002 \tag{2}$$

with $R^2$ of 0.7298.

Desertification degree can be acquired form the equation $I = a * \text{Vegetation} - \text{Albedo}$, where $I$ is referred to as desertification degree index, $a$ is identified by slope coefficient of Eq. (2). In the present study, the value of $a$ is 0.225. By the Jenks natural break method (George 1967), the value of $I$ is divided into five degrees, that is, non-desertification, mild desertification, moderate desertification, severe desertification and extremely severe desertification of the five degrees, mild and moderate desertification refers to that the vegetation coverage is within 31–50 %. In this degree, zonal elite plants begin to decrease, plant components change, xerophytic plants increase and brushwood and sand dune occur. The vegetation coverage of moderate desertification reaches 11–30 %. In this degree, xerophytic plants and psammophytes increase, hard shrub and small sand dune occur and there is widely distributed coarsening gravel surface. Severe desertification vegetation coverage is ≥10 %. The main plants in this degree are psammophytes. There is almost no vegetation in the very severely desertification. Table 2 presents $I$ values of different types of desertification. Little difference of I value exists in the same type of desertification. So, $I$ value may reflect the regional land desertification process. Figure 8 shows the density segmentation image of $I$ value in the whole image A-V feature space. Figure 9 reveals the hierarchical graph of the corresponding desertification.

The evaluation results with the raster form are input into GIS software to make a statistic analysis of area. The results are presented in Table 2. According to Fig. 9 and Table 2, desertification land in the research area of the present study reaches 16,559.12 km$^2$, including 8,872.83 km$^2$ of severe or more severe desertification which

**Table 2** *I* values of different desertification land and classification of desertification

| Desertification type | $I$ | Pixel (number) | Area (km$^2$) | Coverage (%) |
|---|---|---|---|---|
| Non-desertification | 15.645 | 1,672,939 | 1,505.65 | 8.33 |
| Mild desertification | 11.076 | 3,089,489 | 2,780.54 | 15.39 |
| Moderate desertification | 4.668 | 5,450,838 | 4,905.75 | 27.16 |
| Severe desertification | −1.759 | 4,410,312 | 3,969.28 | 21.97 |
| Extremely severe desertification | −4.183 | 5,448,383 | 4,903.54 | 27.14 |

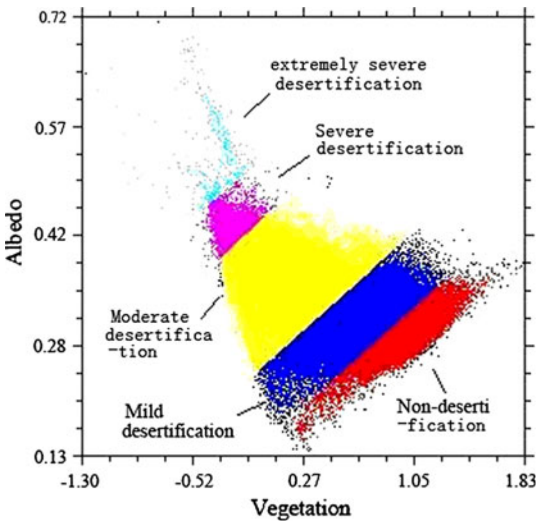


**Fig. 8** Density segmentation map of $I$ value in A-V feature space

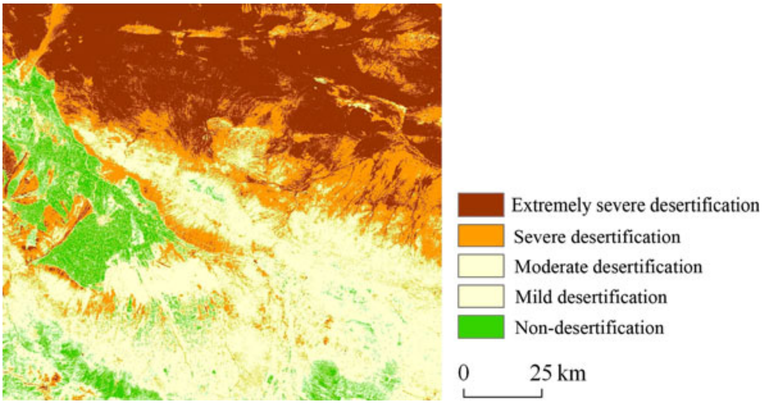


**Fig. 9** Desertification classification map

nearly takes up half the total area of the study area. Therefore, it can be seen that desertification in this area is very serious in 2010. It should be noticed that the extremely severe desertification land surrounding oasis and Heihe River has formed a half surrounding shape which will cause a great threat to the ecological security of oasis. Thus, there areas should be the key regions to prevent desertification. Specially, Ganzhou–Linze–Gaotai oasis surrounded by desertification land shows a patchy shape, which is particularly noticeable.

## 3.3 Verification of evaluation results

The authors in 2010 took four field samplings from July to October for accuracy evaluation and collected the latest categorical managed data and various thematic maps. According to the important degree of different desertification land, the authors randomly selected 5 desertification types and 200 pixels in the remote sensing images to conduct a verification

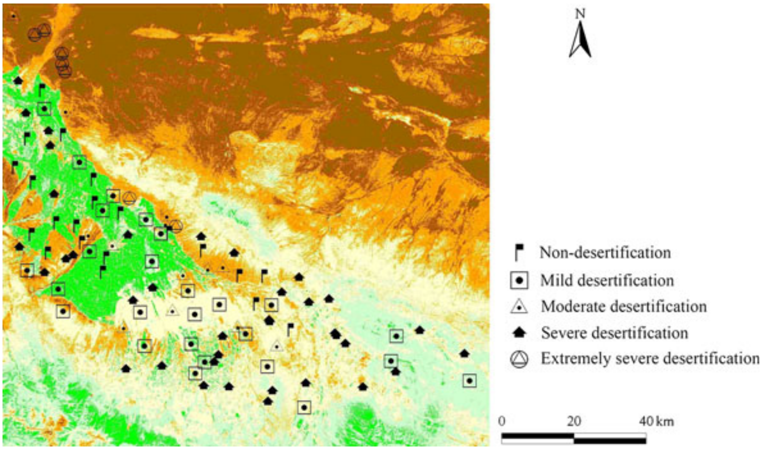


**Fig. 10** Verification diagram of distribution points in research areas

experiment. Considering accessibility of traffic and homogeneity of sampling, the present study focuses on various highways as the main investigation lines. At last, 104 highways located in the southwest part of the research area are chosen as the pixels for accuracy verification (Fig. 10). After comprising the evaluation results of desertification with the sampling data from field areas, a confusion matrix is built. Based on the matrix, it can be seen that the correctly evaluated points are 94, the overall precision reaches 90.3 % and $\kappa$ coefficient is 0.873. The extracting accuracy of non-desertification reaches 100 %, while the extracting accuracy of moderate desertification is only 83.7 % which is the lowest one. The research results show that it is a feasible way to make use of linear spectral mixture analysis and A-V feature space to evaluate desertification.

## 4 Conclusions and discussions

The present study adopts linear spectral mixture analysis to decompose the TM remote sensing images with the purpose of acquiring the relatively abundant distribution of vegetation, bare soil and water components. Based on soil surface albedo, the author constructs a desertification remote monitoring model in Albedo-Vegetation feature space and takes an experimental study in the regions surrounding middle reach of Heihe River. The results of the present study are shown as follows:

(1) The method based on SMA and A-V feature space takes full advantage of multi-dimension remote sensing information. The index reflects surface coverage of desertification, hydro-thermal combination and its change, which has significant biophysics meaning. And the index, which is simple and easy to acquire and only depend on remote image itself to extract information, helps quantitative analysis and monitoring of desertification.

(2) The mixture pixel phenomenon generally exists in desertification land. The method based on SMA and A-V feature space not only overcomes the shortcomings of the traditional desertification remote sensing analysis which considered the pixel as unit of analysis and neglected the space relationship of endmembers, but also prevents vegetation

index from underestimating the insufficiency of living biomass. Comparing with field investigation, it is high precise and the extent of misjudgment is not big.

(3) Based on the previous researches, the method proposed in this paper mainly depends on statistics analysis. It still needs to be developed in the aspects of biophysics of A-V feature space, remote sensing grading standard and verification of desertification. This paper aims at building an easy, simple and quick methodology for desertification remote sensing monitoring and evaluating, so it only focuses on biomass presented by vegetation components and ignores degeneration of vegetation community and vegetation species. In addition, linear spectrum analysis shows some shortcomings in evaluating accuracy, such as the relatively big decomposition error, the complexity of components combined by non-reflector and shadow region and the subjective error in selecting basic components, all of which deserve further investigation.

**Acknowledgments** This work was supported by the National Nature Science Foundation of China (No. 41061017).

## References

Alfredo DC, Emilio C, Camarasaw A (2002) Satellite remote sensing analysis to monitor desertification processes in the crop-range-land boundary of Argentina. J Arid Environ 52:121–133

Asis AJ, Omasa K (2007) Estimation of vegetation parameter for modeling soil erosion using linear Spectral Mixture Analysis of Landsat ETM data. ISPRS J Photogramm Remote Sens 62:309–324

Becker F, Choudhury BJ (1988) Relative sensitivity of normalized difference vegetation Index (NDVI) and microwave polarization difference index (MPDI) for vegetation and desertification monitoring. Remote Sens Environ 24:297–311

Boardman JW, Kruse FA (1994) Automated spectral analysis: a geological example using AVIRIS data, north Grapevine Mountains, NEVADA. In: Proceedings of ERIM Tenth Thematic Conference on Geologic Remote Sensing, San Antonio, 407–418

Chen Z, Elvidge CD, Groenveld DP (1998) Monitoring of seasonal dynamics of arid land vegetation using AVIRIS data. Remote Sens Environ 65:25–266

Chopping M, Su LH, Rango A, Martonchik JV, Peters DPC, Laliberte A (2008) Remote sensing of woody shrub cover in desert grasslands using MISR with a geometric-optical canopy reflectance model. Remote Sens Environ 112:19–34

Civco DL (1989) Topographic normalization of Landsat thematic mapper digital imagery. Photogramm Eng Remote Sens 55:1303–1309

Diouf A, Lambin EF (2001) Monitoring land-cover changes in semi-arid regions: remote sensing data and field observations in the Ferlo, Senegal. Arid Environ 48:129–148

George FJ (1967) The data model concept in statistical mapping. Int Yearb Cartogr 7:186–190

Gillies RR, Carlson TN, Cui J, Kustas WP, Humes KS (1997) A verification of the 'triangle' method for obtaining surface soil water content and energy fluxes from remote measurements of the normalized difference vegetation index (NDVI) and surface radiant temperature. Int J Remote Sens 18:3145–3166

Hanafi A, Jauffret S (2008) Are long-term vegetation dynamics useful in monitoring and assessing desertification processes in the arid steppe, southern Tunisia. J Arid Environ 72:557–572

Hellden U (1991) Desertification. Time for an assessment. Ambio 20:372–383

Hill J, Stellmes M, Udelhoven T, Sommer ARS (2008) Mediterranean desertification and land degradation: mapping related land use change syndromes based on satellite observations. Glob Planet Change 64:146–157

Hosterta P, Roderb A, Hill J (2003) Coupling spectral unmixing and trend analysis for monitoring of long-term vegetation dynamics in Mediterranean rangelands. Remote Sens Environ 87:183–197

Huang S, Siegert F (2006) Land cover classification optimized to detect areas at risk of desertification in North China based on SPOT VEGETATION imagery. J Arid Environ 67:308–327

Ibrahim FN (1978) Anthropogenic causes of desertification in Western Sudan. Geogr J 2:243–254

Kremer RG, Running SW (1993) Community type differentiation using NOAA/AVHRR data within a sagebrush-steppe ecosystem. Remote Sens Environ 46:311–318

Li BL, Zhou CH (2001) Sandy desertification in west of Northeast China plain in the past 10 years. Acta Geogr Sin 56:307–315 (In Chinese)
Li JT, Pu LT, Ji L (2003) The inspection of environmental desertification using GIS based on MODIS. Bimon Xinjiang Meteorol 26:20–23 (In Chinese)
Li SG, Eugster W, Asanuma J, Kotani A, Davaa G, Oyunbaatar D, Sugita M (2006) Energy partitioning and its biophysical controls above a grazing steppe in central Mongolia. Agric For Meteorol 137:89–106
Li ZF, Li XB, Wei DD, Xu X, Wang H (2010) An assessment of correlation on MODIS-NDVI and EVI with natural vegetation coverage in Northern Hebei Province, China. Procedia Environ Sci 2:964–969
Liang S (2000) Narrowband to broadband conversions of land surface albedo: I. Algorithms. Remote Sens Environ 76:213–238
Malo AR, Nicholson SE (1990) A study of rainfall and vegetation dynamics in the African Sahel using normalised difference vegetation index. J Arid Environ 19:1–24
Nicholson SE, Tucker CJ, Ba MB (1998) Desertification, drought and surface vegetation: an example from the West African Sahel. Bull Am Meteorol Soc 79:815–829
Paisley ECI, Lancaster N, Gaddis LR, Greelye R (1991) Discrimination of active and inactive sand from remote sensing: Kelso Dunes, Mojave Desert, California. Remote Sens Environ 37:153–166
Pu RL, Gong P, Michishita R, Sasagawa T (2008) Spectral mixture analysis for mapping abundance of urban surface components from the Terra/ASTER data. Remote Sens Environ 87:939–954
Ridd MK (1995) Exploring a V-I-S(vegetation-impervious surface-soil) model for urban ecosystem analysis through remote sensing: comparative anatomy for cities. Int J Remote Sens 16:2165–2185
Santini M, Caccamo G, Laurenti A, Noce S, Valentini R (2010) A multi-component GIS framework for desertification risk assessment by an integrated index. Appl Geogr 30:394–415
Small C (2001) Estimation of urban vegetation abundance by spectral mixture analysis. Int J Remote Sens 22:1305–1334
Smith MO, Ustin SL, Adams JB, Gillespie AR (1990) Vegetation in deserts: I. A regional measure of abundance from multispectral images. Remote Sens Environ 31:1–26
Sonnenschein R, Kuemmerle T, Udelhoven T, Stellmes M, Hostert P (2011) Differences in Landsat-based trend analyses in drylands due to the choice of vegetation estimate. Remote Sens Environ 115(6):1408–1420
Tripathy GK, Ghosh TK, Shah SD (1996) Monitoring of desertification process in Karnataka state of India using multi-temporal remote sensing and ancillary information using GIS. Int J Remote Sens 17:2243–2257
Verstraete M, Pinty B (1996) Designing optimal spectral indexes for remote sensing applications. Remote Sens Environ 34:1254–1265
Wessels KJ, Prince SD, Frost PE, Zyl DV (2004) Assessing the effects of human-induced land degradation in the former homelands of northern South Africa with a 1 km AVHRR NDVI time-series. Remote Sens Environ 91:47–67
Wu J, Peng DL (2009) Progress on remote sensing-based desertification assessment. World For Res 22:34–39 (In Chinese)
Wu JD, Wang D, Bauer ME (2007) Assessing broadband vegetation indices and QuickBird data in estimating leaf area index of corn and potato canopies. Field Crop Res 102:33–42
Xu DY, Kang XW, Zhuang DF, Pan JJ (2010) Multi-scale quantitative assessment of the relative roles of climate change and human activities in desertification—a case study of the Ordos Plateau, China. J Arid Environ 74:498–507
Xue X, Guo J, Han BS, Sun QW, Liu LC (2009) The effect of climate warming and permafrost thaw on desertification in the Qinghai–Tibetan Plateau. Geomorphology 108:182–190
Yan CZ, Song X, Zhou YM, Duan HC, Li S (2009) Assessment of aeolian desertification trends from 1975's to 2005's in the watershed of the Longyangxia Reservoir in the upper reaches of China's Yellow River. Geomorphology 112:205–211
Yuan F, Marvin E (2007) Comparison of impervious surface area and normalized difference vegetation index as indicators of surface urban heat island effects in Landsat imagery. Remote Sens Environ 206:375–386
Zeng YN, Feng ZD, Xiang NP (2005) The remote sensing synthetic index model for desertification detection. Remote Sens Land Resour 16:40–44 (In Chinese)
Zeng YN, Xiang NP, Feng ZD (2006) Albedo-NDVI space and remote sensing synthesis index models for desertification monitoring. Sci Geogr Sin 26:75–81 (In Chinese)